

## PAPER

[View Article Online](#)  
[View Journal](#) | [View Issue](#)Cite this: *Polym. Chem.*, 2025, **16**, 1813

## The origin of the thermally stable white-light emission property of POSS-conjugated polymer hybrid films†

Satoru Saotome,<sup>a</sup> Masayuki Gon <sup>a,b</sup> and Kazuo Tanaka <sup>\*a,b</sup>

We have previously reported thermally stable white-light luminescence from polymer hybrid films consisting of tetraphenylethene (TPE)-tethered polyhedral oligomeric silsesquioxane (POSS) and poly(1,4-phenylenevinylene) (PPV). We observed that the intensity ratios between the dual emission bands from the POSS and the conjugated polymer, and thus the color balance, were maintained even in the higher-temperature region. In this paper, the origin of the thermally stable dual-emission properties of these white-light-emitting hybrid films is investigated using a series of POSS derivatives with different tethered luminophores and various conjugated polymer matrices. We obtained homogeneous hybrid films and revealed that one of the key factors for the expression of dual-emission properties is the relationship between the photoluminescence quantum yields of the energy donors (fillers) ( $\Phi_D$ ) and acceptors (polymers) ( $\Phi_A$ ). When the emission quantum yield of either the donor or acceptor molecules is high, only an emission band originating from the molecule with the higher emission quantum yield can be observed. Dual emission from both the donor and acceptor is detectable only when the  $\Phi_D$  is as high as the  $\Phi_A$  or slightly higher than the  $\Phi_A$ . Based on these findings, we have demonstrated a logical design for dual-emissive materials. We also found that the affinity between POSS and polymers is responsible for maintaining the emission color balance at high temperatures. It was observed that POSS substituted with bulky groups can hybridize with conjugated polymer chains, and that the thermal behavior of the polymer is dominated by the POSS. As a result, the thermal stability can be enhanced. We revealed the origin of the thermally stable white-light luminescence properties of POSS hybrids based on two aspects.

Received 14th February 2025,

Accepted 14th March 2025

DOI: 10.1039/d5py00144g

[rsc.li/polymers](https://rsc.li/polymers)

## Introduction

$\pi$ -Conjugated polymers have attracted attention as a platform for constructing modern optoelectronic materials owing to their unique material, electrical and optical properties.<sup>1–4</sup> However, the durability of organic materials including conjugated polymers is generally lower than that of inorganics. Therefore, it is still strongly required to reinforce the durability and extend the lifetimes of organic devices. To meet these demands, we have focused on the formation of hybrid materials with polyhedral oligomeric silsesquioxane (POSS).<sup>5</sup> POSS is an organic–inorganic hybrid molecule consisting of a cubic silica core and organic substituents at eight vertices.<sup>6–14</sup>

By connecting organic dyes to POSS, various functional optical materials and sensors can be created.<sup>15–26</sup> In addition, the thermal stability of the dyes can be enhanced.<sup>27–29</sup> Furthermore, by selecting appropriate substituents, it is possible to tune various physical properties, such as miscibility in polymer matrices. In particular, the thermal stability of polymer matrices can be enhanced by simple mixing with POSS because of the suppression of molecular motions by POSS.<sup>30–38</sup> Some POSS derivatives can even show high miscibility with  $\pi$ -conjugated polymers, and the resulting polymer hybrids can act as thermally stable luminescent materials.<sup>39–43</sup> Therefore, we have regarded POSS derivatives as a versatile element-block, which is a minimum functional unit containing a heteroatom, for creating designable hybrid materials through facile preparation methods.<sup>44–49</sup>

White-light-emitting materials are versatile for a variety of applications, such as surface light source illuminators that cast few shadows and lightweight car lamps in motor vehicles.<sup>50</sup> There are several strategies for preparing white-light-luminescent materials based on dye-encapsulated micelles<sup>51–54</sup> or vesicles,<sup>55–57</sup> hybrids containing various

<sup>a</sup>Department of Polymer Chemistry, Graduate School of Engineering, Kyoto University, Nishikyo-ku, Katsura, Kyoto 615-8510, Japan.

E-mail: [tanaka@poly.synchem.kyoto-u.ac.jp](mailto:tanaka@poly.synchem.kyoto-u.ac.jp)

<sup>b</sup>Department of Technology and Ecology, Graduate School of Global Environmental Studies, Kyoto University, Katsura, Nishikyo-ku, Kyoto 615-8510, Japan

† Electronic supplementary information (ESI) available. See DOI: <https://doi.org/10.1039/d5py00144g>



dyes,<sup>58–62</sup> fixation into gels,<sup>63–66</sup> and arrangement with metal-organic frameworks.<sup>67–72</sup> To induce white-light emission, it is essential to mix two or more luminophores in a single material and preserve their luminescence properties in the condensed state of the material. In these multiple-dye-doped materials, critical phase separation occasionally occurs during manufacturing or at the elevated temperatures caused by device operation. Therefore, it is still challenging to enhance the thermal durability and suppress the degradation of white-light luminescence at high temperature.

In a previous report, we demonstrated that a hybrid film composed of 10 wt% poly[2-methoxy-5-(2-ethylhexyloxy)-1,4-phenylenevinylene] (**MEH-PPV**) and 90 wt% tetraphenylethene-tethered POSS (**TPE-POSS**) exhibited white-light luminescence consisting of dual-emission properties originating from the emission band of **TPE-POSS** and that of **MEH-PPV**.<sup>43</sup> In particular, the hybrid film retained white-light luminescence even at high temperature without unexpected changes in the intensity ratios of the emission bands. Although we observed these intriguing thermo-optical properties of POSS hybrid materials, the origin of these unique properties was unclear. To achieve control of their optical properties and the further improvement of their thermal stability, it is essential to comprehend the mechanism and explore further combinations of POSS derivatives and conjugated polymers.

In this report, we prepared hybrid films containing various combinations of a series of luminophore-tethered POSS fillers and conjugated polymer matrices. From optical measurements, we clarified the rule for obtaining dual-emission to produce white-light emission. Based on this information, we demonstrated how to predict optical characteristics based on the optical data of the components. Moreover, from thermal analyses, we obtained the structure–property relationship for

explaining the thermal stability of white-light emission. Based on the optical and thermal studies, we propose the origin of the thermally stable white-light emission of POSS-conjugated polymer hybrids.

## Results and discussion

### Synthesis and sample preparation

The hybrid films were prepared according to the following procedure. Fig. 1 shows the structures of the POSS derivatives (**TPE-POSS**, **DPFL-POSS**, **DPA-POSS**, **TPA-POSS**, **BT-POSS**, **Btz-POSS**, **anth-POSS**, and **DA-POSS**) used in this study. We also prepared *N*-propylmethanimine-modified models for comparison and polymers as a matrix (Fig. S1 and S2†). Each POSS was obtained in high isolated yield through the condensation reaction of octakis(3-aminopropyl) POSS hydrochloride (**Amino-POSS**) and the corresponding aromatic aldehyde.<sup>73,74</sup> The model compounds were prepared using the same condensation reaction between propylamine and the respective aromatic aldehydes. The luminescent  $\pi$ -conjugated polymer **MEH-PPV** was synthesized according to the Gluch route.<sup>43,75,76</sup> Poly(9,9-dihexylfluorene-2,7-diyl) (**PF**) and poly[2,1,3-benzothiadiazole-4,7-diyl(3,3'-didodecyl[2,2'-bithiophene]-5,5'-diyl)] (**PDA**) were synthesized by cross-coupling polymerization. Poly(3-hexylthiophene-2,5-diyl) (**P3HT**) was prepared according to a method in the literature.<sup>77</sup> The molecular weights were determined using size-exclusion chromatography with polystyrene standards and chloroform as an eluent. All polymers had sufficient molecular weights to show good film formability and sufficient length to exclude molecular-weight effects on the electronic properties of the polymers. The structures of all new compounds were confirmed using <sup>1</sup>H, <sup>13</sup>C and

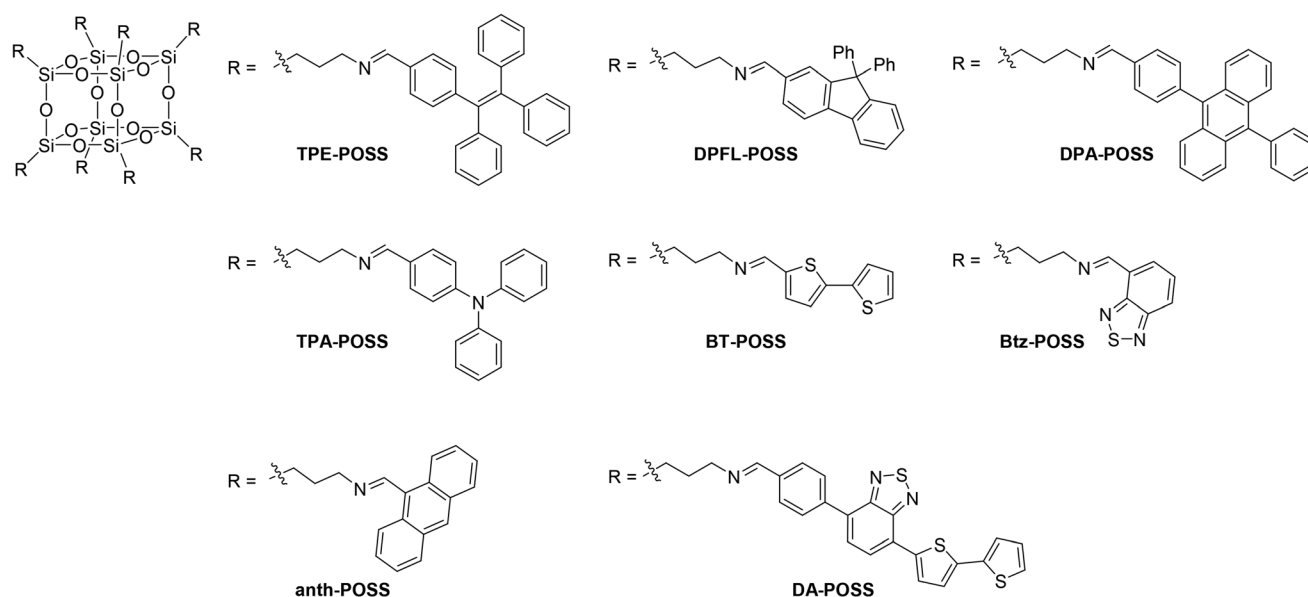


Fig. 1 Chemical structures of POSS derivatives.



$^{29}\text{Si}$  NMR spectroscopy (Charts S1–S41†), high-resolution mass spectrometry and elemental analyses.

Hybrid films were fabricated using a spin-coating method (1000 rpm, 30 s) on quartz substrates (0.9 cm × 5 cm) from the chloroform solutions. The concentration of polymers in chloroform was fixed at 1.0 mg per 300  $\mu\text{L}$ . The concentration of POSS derivatives or model compounds in chloroform was also 1.0 mg per 300  $\mu\text{L}$  for preparing neat films. The optical properties of the POSS derivatives and polymers are summarized in Tables S1 and S2.† The POSS derivatives and polymers are expected to act as energy donors and acceptors, respectively, except for **DA-POSS** and **PF**. For each combination, hybrid films containing 0, 50, 90, and 100 wt% POSS derivatives were prepared. We obtained homogenous thin films, indicating that POSS-conjugated polymer hybrids can be obtained from the various combinations, and used them for further measurements (Fig. S3†). Although the luminophores are connected by imine bonds, which can potentially be hydrolyzed, the hybrid films can be handled and stored stably in air. Owing to the radially arranged hydrophobic luminophores on POSS, degradation could be suppressed by the restricted accessibility of water molecules.

### Evaluation of dual-emission properties

For almost all the combinations, the hybrid films showed brighter emission with higher POSS content (Table 1, Fig. S4 and S5†). Some combinations exhibited dual emission at 90 wt% POSS content, while others showed only POSS emission or polymer emission. **MEH-PPV** showed dual emission in the presence of **TPA-POSS**, whereas only polymer emission was observed from the **BT-POSS** hybrids. **P3HT** showed dual emission with **BT-POSS**, although only POSS emission was detected from the **TPA-POSS** hybrids. These differences seemed to result from the differences between the quantum yields of the components. To examine the relationships between the dual emission properties and  $\Phi_{\text{film}}$ , the optical properties of the film samples for each combination were investigated (Fig. 2). The data can be classified into three areas: I ( $\Phi_{\text{POSS}} > \Phi_{\text{polymer}}$ ), II ( $\Phi_{\text{POSS}} \cong \Phi_{\text{polymer}}$ ) and III ( $\Phi_{\text{POSS}} < \Phi_{\text{polymer}}$ ). In area I, the hybrid films showed only the emission band of POSS even when they contained 90 wt% POSS. According to our previous report, POSS should form domains in polymer matrices.<sup>43</sup> As a result, energy transfer should be disturbed. In area III, only the emission band attributable to the polymer was observed regardless of the POSS content.

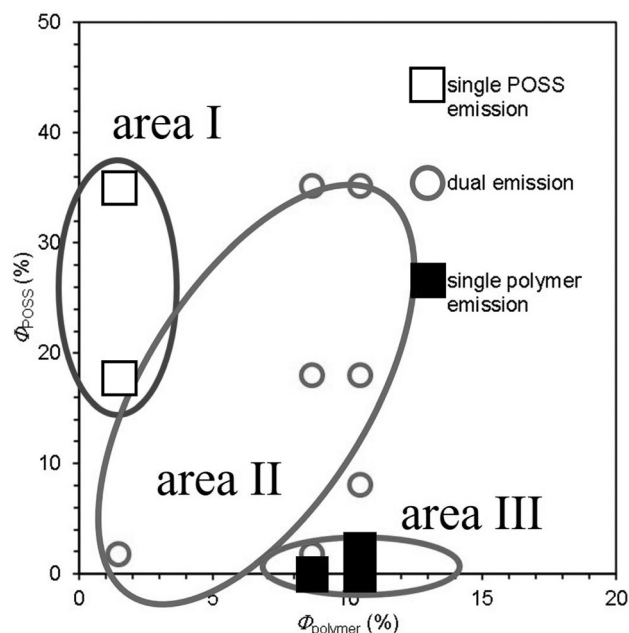


**Fig. 2** Plots of the emission efficiencies of hybrid films containing POSSs. The horizontal and vertical axes represent  $\Phi_{\text{film,polymer}}$  and  $\Phi_{\text{film,POSS}}$ , respectively. The samples in area II showed dual emission from both the POSS and polymer. The samples in areas I and III showed emission from only the POSS or only the polymer, respectively.

This is because the luminescence ability of the energy donor should be too weak to exhibit its own emission after energy transfer. In area II, it should be noted that dual emission from both the POSS and the polymer was detected when the POSS content was over 50 wt% (**PDA** or **P3HT** hybrid films) or 90 wt% (**MEH-PPV** hybrid films). It is suggested that, similarly to the samples categorized in area I, the energy transfer from POSS should be suppressed, and the emission from POSS can be detected.

To investigate the influence of POSS on luminescent properties, hybrid films were prepared with model compounds and other polymer matrices (Fig. S6–S8, Tables S3 and S4†). Using the same method as that for preparing POSS hybrids, film samples containing 0, 50, 90, and 100 wt% of each model compound were fabricated. Interestingly, the films showed dual emission or only polymer emission. In light of the fact that the hybrid films containing POSS tended to exhibit dual emission or only POSS emission, these results can also be

**Table 1** Luminescence behaviors of the combinations of POSSs and polymers<sup>a</sup>

	TPE-POSS	TPA-POSS	DPA-POSS	BT-POSS	anth-POSS	DPFL-POSS	Btz-POSS
<b>MEH-PPV</b>	○	○	○	■	■	■	■
<b>PDA</b>	○	○	— <sup>b</sup>	○	— <sup>b</sup>	— <sup>b</sup>	— <sup>b</sup>
<b>P3HT</b>	□	□	— <sup>b</sup>	○	— <sup>b</sup>	— <sup>b</sup>	— <sup>b</sup>

<sup>a</sup> Circles indicate combinations that showed dual emission from both the POSS and polymer. White and black squares indicate combinations that showed the emission from only the POSS or only the polymer, respectively. Various contents of POSS (0, 50, 90, and 100 wt%) were loaded for testing each combination. <sup>b</sup> The test was not conducted.



explained by the formation of domain structures, similar to our previous results.<sup>43</sup> In the case of the hybrids including model compounds, the luminophores and polymer chains can interact. As a result, efficient energy transfer should proceed in the film, resulting in emission annihilation of a single luminophore molecule. In contrast, the bulky structure of the POSS core makes it likely that each luminophore will be isolated from the polymer chains at the molecular level. Moreover, POSS forms domain structures with sizes of several tens of nanometers in the polymer matrices.<sup>43</sup> Consequently, in the presence of POSS, energy transfer should be restricted in the films, and dual emission can be induced.

Next, we also investigated reverse energy transfer between **PF** and **DA-POSS**, which should act as an energy donor and acceptor, respectively. The values of  $\Phi_{\text{PF, film}}$  and  $\Phi_{\text{DA-POSS, film}}$  are 13% and 2%, respectively, and this combination is found in area II in Fig. 2, meaning that white-light dual emission can be expected. To confirm the validity of this estimation, the hybrid films were prepared using the same method as previous examples with variable content of **DA-POSS** (0, 10, 25, 50, 75, 90, and 100 wt%), and their optical properties were investigated. Accordingly, as seen in Fig. 3, white-light luminescence was detected from the film containing 10 wt% of **DA-POSS**. This result indicates that dual emission can be realized if the balance of  $\Phi_{\text{donor, film}}$  and  $\Phi_{\text{acceptor, film}}$  is optimized.

### Influence of thermal stability of color balance

First, to investigate the contribution of each material to the thermal stability of the color balance of the white-light emission reported in the previous study, we evaluated the effect of thermal stability by replacing the individual components in the hybrid film based on **TPE-POSS** and **MEH-PPV**. Instead of **TPE-POSS** or **MEH-PPV**, **TPA-POSS** or **PDA** was used, respectively. The emission spectrum with changing temperature was

monitored, and the emission intensities from the POSS and polymer moieties were plotted *versus* temperature. As shown in Fig. 4, the hybrid film with 90 wt% **TPA-POSS** and 10 wt% **MEH-PPV** exhibited low thermal stability in terms of color balance. The emission bands decreased individually with heating. Conversely, the film containing 90 wt% **TPE-POSS** and 10 wt% **PDA** showed the desired thermally stable emission behavior (Fig. 5). The emission of **TPE-POSS** and **PDA** attenuated in a concerted fashion in the film, similar to the film consisting of **TPE-POSS** and **MEH-PPV** in the previous report (Fig. S9†).<sup>43</sup> The partial emission peak shift of **PDA** around 676 nm with increasing temperature should be attributed to the intramolecular conformational change of the polymer main-chain. As the intermolecular main-chain interactions are suppressed by bulky POSS, the spectral changes should be small and hardly affect the color balance of the white-light emission. In the hybrid film with the model compound, the concerted decrease in the emission intensity with increasing temperature was not observed (Fig. S10 and S11†), similarly to in our previous report.<sup>43</sup> These results imply that **TPE-POSS** could play an important role in maintaining color balance at high temperatures.

**TPE-POSS** has several distinctive characteristics, namely, a bulky steric structure, aggregation-induced emission properties, and affinity with  $\pi$  surfaces.<sup>43</sup> To elucidate which properties were important to the thermally stable color balance, other POSSs with one of the same properties as **TPE-POSS** were hybridized with **MEH-PPV**, and their optical and thermal properties were evaluated. **DPFL-POSS**, which has a bulky steric structure similar to that of **TPE-POSS**, and **BT-POSS**, which is expected to have a higher affinity with  $\pi$  surfaces than **TPE-POSS**, were applied. The color balance of the hybrid films with changing temperature was monitored to clarify the POSS substituent effect on thermal stability.

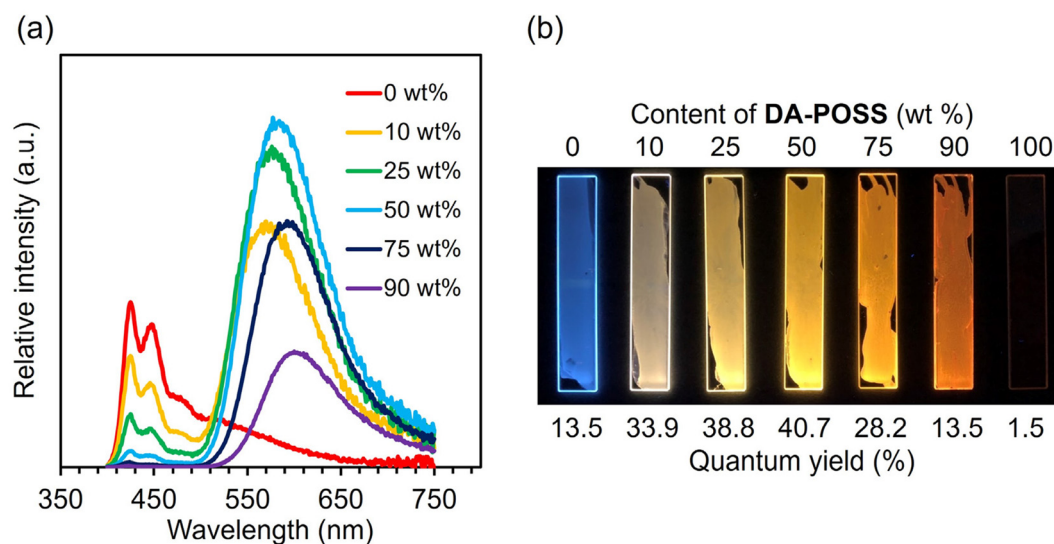


**Fig. 3** (a) Relative photoluminescence spectra of **PF** and **DA-POSS** hybrid films excited at  $\lambda_{\text{abs, PF}}$  (385 nm). Numbers in the legend indicate the content ratios of **DA-POSS**. (b) Photos of **PF** and **DA-POSS** hybrid films irradiated by a UV lamp (365 nm).





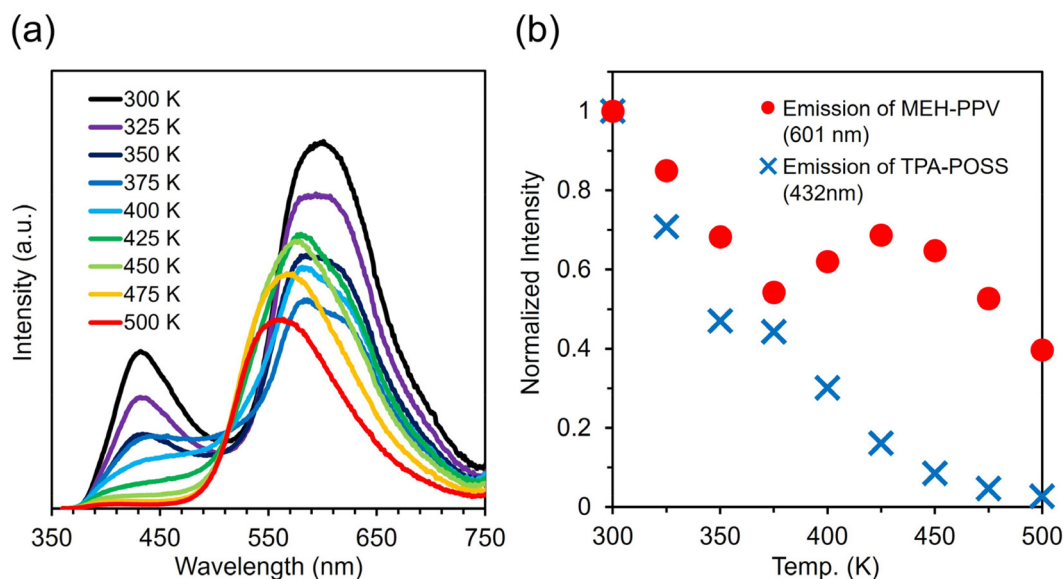


Fig. 4 (a) Variable-temperature emission spectra with excitation at 350 nm and (b) intensity ratios at 432 nm for TPA-POSS and 601 nm for MEH-PPV in the hybrid film containing 10 wt% MEH-PPV and 90 wt% TPA-POSS.

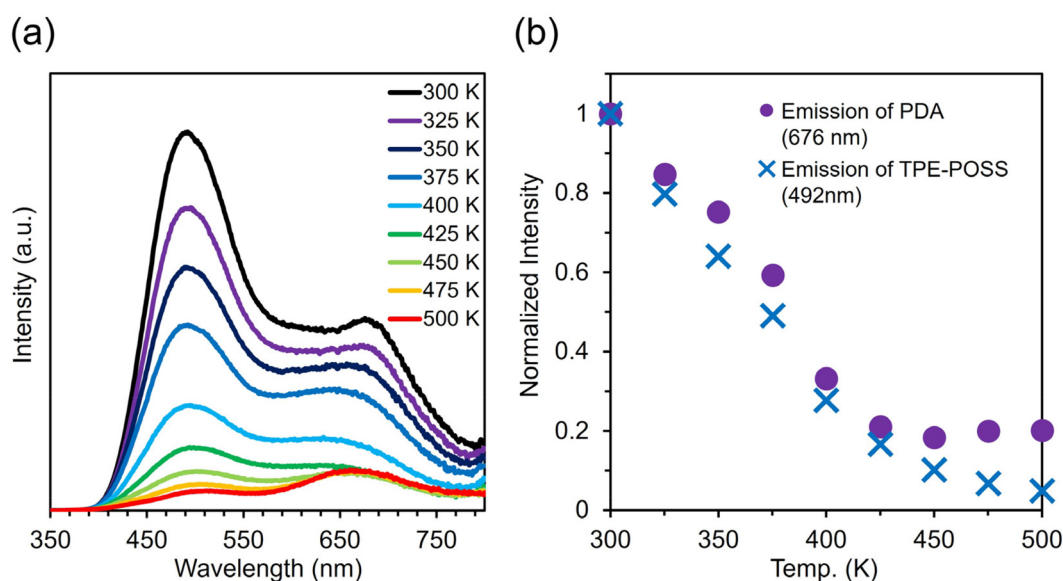


Fig. 5 (a) Variable-temperature emission spectra with excitation at 330 nm and (b) intensity ratios at 492 nm for TPE-POSS and 676 nm for PDA in the hybrid film containing 10 wt% PDA and 90 wt% TPE-POSS.

Fig. S12<sup>†</sup> shows the emission spectra and peak-top decay plots at various temperatures for hybrid films containing 90 wt% BT-POSS and 10 wt% MEH-PPV. The emission of MEH-PPV decreased with increasing temperature until 375 K and then increased. This behavior was similar to the emission decay of MEH-PPV in the neat film (Fig. S13<sup>†</sup>) and TPA-POSS hybrid film (Fig. 4). In these films, the emission intensities decreased or remained the same until 375 K, then increased until 425 K, and then decreased again. This behavior indicates that MEH-PPV retains its bulk characteristics, and that

MEH-PPV and POSSs exhibit their optical thermal properties individually. Hence, these materials do not preserve the color balance at high temperature.

In the case of the hybrid film containing 90 wt% DPFL-POSS and 10 wt% MEH-PPV, due to the almost complete lack of luminescence from DPFL-POSS, we were unable to plot the peak tops of DPFL-POSS emission (Fig. S14<sup>†</sup>). In this film, the emission of MEH-PPV decreased monotonically. This decrease is similar to that of the TPE-POSS hybrid film, as shown in Fig. S9<sup>†</sup>. The emission of MEH-PPV in the TPE-POSS



hybrid film decreased more drastically than that in the **DPFL-POSS** hybrid film. This is explained by its energy donation ability. As **TPE-POSS** is more luminescent than **DPFL-POSS**, **MEH-PPV** has a relatively higher emission intensity at 300 K in the **TPE-POSS** hybrid film than in the **DPFL-POSS** hybrid film. As a result, the difference between its intensity at 300 K and 500 K is larger compared to that of the **TPE-POSS** hybrid. Based on the similarity between the **TPE-POSS** and **DPFL-POSS** hybrid film, the bulky steric substituents of the POSS should be regarded as the key to the thermally stable color balance. In the hybrid film, **MEH-PPV** should be isolated by the surrounding excess bulky POSS, and thus, its bulk characteristics as a polymer are no longer observed. Therefore, it is likely that the molecular motion of **MEH-PPV** should be restricted by the POSS. At high temperatures, it is proposed that the emission intensities of **MEH-PPV** and **TPE-POSS** could decrease concertedly when molecular motions occur in the POSS units due to heating.

To gather information on the isolation effect on the polymer chains, differential scanning calorimetry (DSC) measurements were performed. The films were fabricated by the drop-casting method. Fig. S15† shows the DSC curves of the **MEH-PPV** neat film and hybrid films containing 10 wt% **MEH-PPV** and 90 wt% POSS derivatives. The shape of the endothermic peak in the DSC curve, which is assigned to the glass transition, was distinctive. Compared with the **MEH-PPV** neat film, the hybrid films with non-bulky POSSs such as **TPA-POSS** and **BT-POSS** showed sharp peaks, indicating that the relaxation time of **MEH-PPV** should be little affected by the POSS. In contrast, relatively broad endothermic peaks were observed for the hybrid films containing the bulky POSS derivatives such as **TPE-POSS** and **DPFL-POSS**, meaning that the distribution of the relaxation time should be widened due to hybridization. The fact that the difference in the relaxation times of the polymers is dispersed means that the properties of the polymer chains are not averaged, in other words, the **MEH-PPV** chains could be well separated in these hybrid films.

To estimate the affinity between a polymer and filler, the Flory–Huggins interaction parameters ( $\chi$ ) are often used.<sup>78–87</sup> As has been conducted in several studies, the interaction parameters were calculated from the contact angles (Tables S5–S7 and Fig. S16†).<sup>81–83</sup> To qualitatively discuss the affinity between the POSS derivatives and **MEH-PPV**, we estimated the interaction parameter using this indirect method. The trend in the interaction parameters reasonably explains the relationship between the affinity and bulkiness of the substituents on the POSS. The derivatives having bulky substituents, including **TPE-POSS**, **DPFL-POSS** and **DPA-POSS**, show relatively smaller  $\chi_{\text{MEH-PPV,POSS}}$  values, while those with less-bulky substituents, including **TPA-POSS**, **BT-POSS**, **anth-POSS** and **Btz-POSS**, exhibit larger  $\chi_{\text{MEH-PPV,POSS}}$  values. Based on these results, it is suggested that bulky substituents show a positive effect in improving affinity toward polymer chains, leading to the isolation of the polymer chains (Fig. 6). In this state, the molecular motions of the polymer chains are dominated by POSS, and therefore, the emissions of the polymer chains can be annihilated correspondingly with the decrease in the emission intensity of the POSS by heating. Moreover, it should be noted that the POSS derivatives having bulky substituents are favorable for controlling the thermo-optical properties of the polymer by hybridization.

In summary, the structure–property relationship for the thermo-optical properties in POSS hybrid materials is explained as follows. As shown in Fig. 6, the bulky substituents on the POSS derivative promote the hybridization of the POSS with polymer chains. In this state, the polymer chains are isolated from each other, and the properties of the bulk materials should no longer be observed. In particular, the degree of molecular motion is determined by the surrounding POSS molecules. Therefore, the thermal decay of the emission intensity from the polymer chains proceeds monotonically, corresponding with that of the POSS, and the ratio between their emission intensity is maintained during the luminescence decay of the overall hybrid material. Thus, the hybrid film

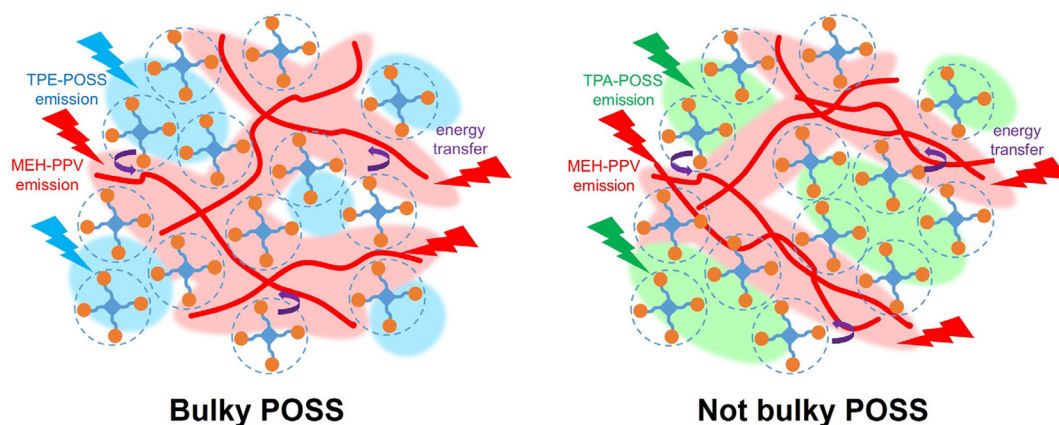


Fig. 6 Schematic models of hybrid films containing a bulky-group-substituted POSS (such as **TPE-POSS**) and a less-bulky-group-substituted POSS (such as **TPA-POSS**).



maintains the color balance of the white emission even at high temperatures.

## Conclusion

In this study, the key factors for the unique phenomenon of thermally stable white-light luminescence were revealed using two approaches: the origin of the dual emission and that of the thermally stable color balance. The balance between the luminescence quantum yields of the POSS and the polymer, which can act as a donor and an acceptor in the energy transfer system, respectively, has been found to be important. When one is much larger than another, emission is only observed from one component. If both values are similar, dual emission from both the POSS and polymer components can be detected. In other words, the dual-emission properties of the hybrid materials can be predicted based on the relative magnitudes of  $\Phi_{\text{POSS, film}}$  and  $\Phi_{\text{polymer, film}}$ . We also found that the affinity between the POSS and polymers is the key to maintaining the emission color balance at high temperatures. DSC measurements revealed that POSS derivatives containing bulky substituents have good affinity with polymers. When such POSS derivatives are hybridized with a polymer, the thermal behavior of the polymer is dominated by the POSS. Polymers hybridized with a bulky POSS cannot behave as bulk materials and are influenced by the surrounding POSS. The emission from the polymer decreases monotonically upon heating, and the behavior corresponds to the decay of the POSS. As a result, the hybrid film, as a single material, decreases in emission without change in its emission color. Flory–Huggins interaction parameters ( $\chi$ ) are available for estimating the affinity of several POSSs toward MEH-PPV. This means that by using  $\chi_{\text{POSS, polymers}}$  it is possible to predict whether a hybrid material will maintain its color balance when heated. Our findings may have potential applications in developing thermally stable light emitters as well as for tailoring the properties of materials based on hybrids by designing POSS structures.

## Data availability

The data supporting this article have been included as part of the ESI.†

## Conflicts of interest

There are no conflicts to declare.

## Acknowledgements

This work was partially supported by the ENEOS Tonengeneral Research/Development Encouragement & Scholarship Foundation, Japan (for M. G.) and JSPS KAKENHI Grant Numbers 24K01570 (for K. T.).

## References

- 1 J. H. Burroughes, D. D. C. Bradley, A. R. Brown, R. N. Marks, K. Mackay, R. H. Friend, P. L. Burns and A. B. Holmes, *Nature*, 1990, **347**, 539–541.
- 2 H. Sirringhaus, P. J. Brown, R. H. Friend, M. M. Nielsen, K. Bechgaard, B. M. W. Langeveld-Voss, A. J. H. Spiering, R. A. J. Janssen, E. W. Meijer, P. Herwig and D. M. de Leeuw, *Nature*, 1999, **401**, 685–688.
- 3 K. Mahesh, S. Karpagam and F. Goubard, *EXPRESS Polym. Lett.*, 2018, **12**, 238–255.
- 4 A. C. Grimsdale, K. Leok Chan, R. E. Martin, P. G. Jokisz and A. B. Holmes, *Chem. Rev.*, 2009, **109**, 897–1091.
- 5 K. Tanaka and Y. Chujo, *J. Mater. Chem.*, 2012, **22**, 1733–1746.
- 6 D. B. Cordes, P. D. Lickiss and F. Rataboul, *Chem. Rev.*, 2010, **110**, 2081–2173.
- 7 J. J. Schwab and J. D. Lichtenhan, *Appl. Organomet. Chem.*, 1998, **12**, 707–713.
- 8 F. K. Wang, X. Lu and C. He, *J. Mater. Chem.*, 2011, **21**, 2775–2782.
- 9 K. Naka and Y. Irie, *Polym. Int.*, 2017, **66**, 187–194.
- 10 Y. Kaneko, *Chem. Rec.*, 2023, **23**, e202200291.
- 11 Y. Liu, K. Koizumi, N. Takeda, M. Unno and A. Ouali, *Inorg. Chem.*, 2022, **61**, 1495–1503.
- 12 R. Kajiya, H. Wada, K. Kuroda and A. Shimojima, *Chem. Lett.*, 2020, **49**, 327–329.
- 13 H. Sakai, T.-M. Yung, T. Mure, N. Kurono, S. Fujii, Y. Nakamura, T. Hayakawa, M.-C. Li and T. Hirai, *JACS Au*, 2023, **3**, 2698–2702.
- 14 S. Morimoto, H. Imoto and K. Naka, *Chem. Commun.*, 2017, **53**, 9273–9276.
- 15 M. Gon, K. Tanaka and Y. Chujo, *Chem. – Asian J.*, 2022, **17**, e202200144.
- 16 H. Narikiyo, D. Iizuka, M. Gon, K. Tanaka and Y. Chujo, *Eur. J. Inorg. Chem.*, 2025, **28**, e202400731.
- 17 H. Narikiyo, M. Gon, K. Tanaka and Y. Chujo, *Asian J. Org. Chem.*, 2025, **14**, e202400508.
- 18 H. Narikiyo, T. Kato, M. Gon, K. Tanaka and Y. Chujo, *ChemPhotoChem*, 2025, **9**, e202400273.
- 19 H. Narikiyo, M. Gon, K. Tanaka and Y. Chujo, *Bull. Chem. Soc. Jpn.*, 2024, **97**, uoae066.
- 20 H. Narikiyo, M. Gon, K. Tanaka and Y. Chujo, *Polym. J.*, 2024, **56**, 661–666.
- 21 D. Iizuka, M. Gon, K. Tanaka and Y. Chujo, *Chem. Commun.*, 2022, **58**, 12184–12187.
- 22 D. Iizuka, M. Gon, K. Tanaka and Y. Chujo, *Bull. Chem. Soc. Jpn.*, 2022, **95**, 743–747.
- 23 R. Nakamura, H. Narikiyo, M. Gon, K. Tanaka and Y. Chujo, *Mater. Chem. Front.*, 2019, **3**, 2690–2695.
- 24 H. Narikiyo, M. Gon, K. Tanaka and Y. Chujo, *Mater. Chem. Front.*, 2018, **2**, 1449–1455.
- 25 H. Narikiyo, T. Kakuta, H. Matsuyama, M. Gon, K. Tanaka and Y. Chujo, *Bioorg. Med. Chem.*, 2017, **25**, 3431–3436.
- 26 T. Kakuta, K. Tanaka and Y. Chujo, *J. Mater. Chem. C*, 2015, **3**, 12539–12545.



- 27 K. Sato, M. Gon, K. Tanaka and Y. Chujo, *Bull. Chem. Soc. Jpn.*, 2024, **97**, uoae040.
- 28 M. Gon, K. Sato, K. Tanaka and Y. Chujo, *RSC Adv.*, 2016, **6**, 78652–78660.
- 29 K. Suenaga, K. Tanaka and Y. Chujo, *Chem. – Eur. J.*, 2017, **23**, 1409–1414.
- 30 E. Ayandele, B. Sarkar and P. Alexandridis, *Nanomaterials*, 2012, **2**, 445–475.
- 31 I. Blanco and F. A. Bottino, *Polym. Compos.*, 2013, **34**, 225–232.
- 32 K. Tanaka, S. Adachi and Y. Chujo, *J. Polym. Sci., Part A: Polym. Chem.*, 2010, **48**, 5712–5717.
- 33 J.-H. Jeon, K. Tanaka and Y. Chujo, *J. Polym. Sci., Part A: Polym. Chem.*, 2013, **51**, 3583–3589.
- 34 H. Kozuka, K. Tanaka and Y. Chujo, *Eur. Polym. J.*, 2022, **175**, 111360.
- 35 K. Ueda, K. Tanaka and Y. Chujo, *Polym. J.*, 2020, **52**, 523–528.
- 36 K. Ueda, K. Tanaka and Y. Chujo, *Bull. Chem. Soc. Jpn.*, 2017, **90**, 205–209.
- 37 K. Ueda, K. Tanaka and Y. Chujo, *Polymers*, 2018, **10**, 1332.
- 38 K. Tanaka, H. Kozuka, K. Ueda, J.-H. Jeon and Y. Chujo, *Mater. Lett.*, 2017, **203**, 62–67.
- 39 K. Ueda, K. Tanaka and Y. Chujo, *Polym. J.*, 2016, **48**, 1133–1139.
- 40 K. Ueda, K. Tanaka and Y. Chujo, *Polymers*, 2019, **11**, 44.
- 41 M. Gon, K. Sato, K. Kato, K. Tanaka and Y. Chujo, *Mater. Chem. Front.*, 2019, **3**, 314–320.
- 42 M. Gon, K. Kato, K. Tanaka and Y. Chujo, *Mater. Chem. Front.*, 2019, **3**, 1174–1180.
- 43 M. Gon, S. Saotome, K. Tanaka and Y. Chujo, *ACS Appl. Mater. Interfaces*, 2021, **13**, 12483–12490.
- 44 Y. Chujo and K. Tanaka, *Bull. Chem. Soc. Jpn.*, 2015, **88**, 633–643.
- 45 M. Gon, K. Tanaka and Y. Chujo, *Bull. Chem. Soc. Jpn.*, 2017, **90**, 463–474.
- 46 M. Gon, K. Tanaka and Y. Chujo, *Polym. J.*, 2018, **50**, 109–126.
- 47 K. Tanaka and Y. Chujo, *Polym. J.*, 2020, **52**, 555–566.
- 48 M. Gon, S. Ito, K. Tanaka and Y. Chujo, *Bull. Chem. Soc. Jpn.*, 2021, **94**, 2290–2301.
- 49 K. Tanaka and Y. Chujo, *Polym. J.*, 2023, **55**, 353–364.
- 50 E. Frezza and R. D. Costa, *Adv. Funct. Mater.*, 2020, **30**, 1908176.
- 51 P. Pallavi, B. Sk, P. Ahir and A. Patra, *Chem. – Eur. J.*, 2018, **24**, 1151–1158.
- 52 X. Zhang, D. Görl and F. Würthner, *Chem. Commun.*, 2013, **49**, 8178–8180.
- 53 R. Wang, J. Peng, F. Qiu and Y. Yang, *Chem. Commun.*, 2011, **47**, 2787–2789.
- 54 M. Bälter, S. Li, M. Morimoto, S. Tang, J. Hernando, G. Guirado, M. Irie, F. M. Raymo and J. Andréasson, *Chem. Sci.*, 2016, **7**, 5867–5871.
- 55 X. Zhang, S. Rehm, M. M. Safont-Sempere and F. Würthner, *Nat. Chem.*, 2009, **1**, 623–629.
- 56 J. Huang, Y. Yu, L. Wang, X. Wang, Z. Gu and S. Zhang, *ACS Appl. Mater. Interfaces*, 2017, **9**, 29030–29037.
- 57 P. Xing, Z. Zhao, A. Hao and Y. Zhao, *Chem. Commun.*, 2016, **52**, 1246–1249.
- 58 H.-T. Feng, X. Zheng, X. Gu, M. Chen, J. W. Y. Lam, X. Huang and B. Z. Tang, *Chem. Mater.*, 2018, **30**, 1285–1290.
- 59 X.-L. Ni, S. Chen, Y. Yang and Z. Tao, *J. Am. Chem. Soc.*, 2016, **138**, 6177–6183.
- 60 T. Ono and Y. Hisaeda, *J. Mater. Chem. C*, 2019, **7**, 2829–2842.
- 61 W. Yuan, L. Shu, J. Xu, C. Hua and J. Huang, *ACS Macro Lett.*, 2025, **14**, 51–56.
- 62 X. Li, L. Liu, L. Jia, Z. Lian, J. He, S. Guo, Y. Wang, X. Chen and H. Jiang, *Nat. Commun.*, 2025, **16**, 467.
- 63 D. Podder, S. K. Nandi, S. Sasmal and D. Haldar, *Langmuir*, 2019, **35**, 6453–6459.
- 64 X. Cao, H. Lan, Z. Li, Y. Mao, L. Chen, Y. Wu and T. Yi, *Phys. Chem. Chem. Phys.*, 2015, **17**, 32297–32303.
- 65 P. Bairi, B. Roy, P. Chakraborty and A. K. Nandi, *ACS Appl. Mater. Interfaces*, 2013, **5**, 5478–5485.
- 66 C. Vijayakumar, V. K. Praveen and A. Ajayaghosh, *Adv. Mater.*, 2009, **21**, 2059–2063.
- 67 X.-Y. Liu, K. Xing, Y. Li, C.-K. Tsung and J. Li, *J. Am. Chem. Soc.*, 2019, **141**, 14807–14813.
- 68 Z. Wang, C.-Y. Zhu, J.-T. Mo, P.-Y. Fu, Y.-W. Zhao, S.-Y. Yin, J.-J. Jiang, M. Pan and C.-Y. Su, *Angew. Chem., Int. Ed.*, 2019, **58**, 9752–9757.
- 69 Y.-P. Xia, C.-X. Wang, L.-C. An, D.-S. Zhang, T.-L. Hu, J. Xu, Z. Chang and X.-H. Bu, *Inorg. Chem. Front.*, 2018, **5**, 2868–2874.
- 70 C.-Y. Sun, X.-L. Wang, X. Zhang, C. Qin, P. Li, Z.-M. Su, D.-X. Zhu, G.-G. Shan, K.-Z. Shao, H. Wu and J. Li, *Nat. Commun.*, 2013, **4**, 2717.
- 71 W. Newsome, S. Ayad, J. Cordova, E. W. Reinheimer, A. D. Campiglia, J. K. Harper, K. Hanson and F. J. Uribe-Romo, *J. Am. Chem. Soc.*, 2019, **141**, 11298–11303.
- 72 Q. Yang, W. Wang, Y. Yang, P. Li, X. Yang, F. Bai and B. Zou, *Nat. Commun.*, 2025, **16**, 696.
- 73 H. Imoto, S. Wada and K. Naka, *Chem. Lett.*, 2016, **45**, 1256–1258.
- 74 M. Janeta, L. John, J. Ejfler, T. Lis and S. Szafert, *Dalton Trans.*, 2016, **45**, 12312–12321.
- 75 H.-L. Chow, K.-F. Lin and D.-C. Wang, *J. Polym. Sci., Part B: Polym. Phys.*, 2006, **44**, 62–69.
- 76 H.-L. Chou, K.-F. Lin and D.-C. Wang, *J. Polym. Res.*, 2006, **13**, 79–84.
- 77 R. S. Loewe, S. M. Khersonsky and R. D. McCullough, *Adv. Mater.*, 1999, **11**, 250–253.
- 78 D. R. Kozub, K. Vakhshouri, L. M. Orme, C. Wang, A. Hexemer and E. D. Gomez, *Macromolecules*, 2011, **44**, 5722–5726.
- 79 S. A. Dowland, M. Salvador, J. D. Perea, N. Gasparini, S. Langner, S. Rajoelson, H. H. Ramanitra, B. D. Lindner, A. Osvet, C. J. Brabec, R. C. Hiorns and H.-J. Egelhaaf, *ACS Appl. Mater. Interfaces*, 2017, **9**, 10971–10982.





- 80 P. Westacott, N. D. Treat, J. Martin, J. H. Bannock, J. C. de Mello, M. Chabiny, A. B. Sieval, J. J. Michels and N. Stingelin, *J. Mater. Chem. A*, 2017, **5**, 2689–2700.
- 81 J. Y. Kim, *Macromolecules*, 2019, **52**, 4317–4328.
- 82 J.-H. Kim, A. Gadisa, C. Schaefer, H. Yao, B. R. Gautam, N. Balar, M. Ghasemi, I. Constantinou, F. So, B. T. O'Connor, K. Gundogdu, J. Hou and H. Ade, *J. Mater. Chem. A*, 2017, **5**, 13176–13188.
- 83 S. Nilsson, A. Bernasik, A. Budkowski and E. Moons, *Macromolecules*, 2007, **40**, 8291–8301.
- 84 L. Ye, H. Hu, M. Ghasemi, T. Wang, B. A. Collins, J.-H. Kim, K. Jiang, J. H. Carpenter, H. Li, Z. Li, T. McAfee, J. Zhao, X. Chen, J. L. Y. Lai, T. Ma, J.-L. Bredas, H. Yan and H. Ade, *Nat. Mater.*, 2018, **17**, 253–260.
- 85 E. L. Hynes, J. T. Cabral, A. J. Parnell, P. Gutfreund, R. J. L. Welbourn, A. D. F. Dunbar, D. Môn and A. M. Higgins, *Commun. Phys.*, 2019, **2**, 112.
- 86 K. Milczewska, A. Voelkel and J. Jeczalik, *Macromol. Symp.*, 2003, **194**, 305–312.
- 87 K. Milczewska and A. Voelkel, *J. Appl. Polym. Sci.*, 2008, **107**, 2877–2882.

